(2)

FINAL TECHNICAL REPORT

Project Title:	Negative Electron Affinity for Infrared Detection
Principal Investigator:	Martin A. Gundersen
Agency:	Office of Naval Research
Award No.:	N00014-86-K-0510
Period:	July 1, 1986 - September 30, 1989

Introduction

This study has extensively examined the optical properties of GaP, and concentrated upon the optical bistability of GaP device and a gallium phosphide infrared detector based on linear upconversion .

Optical Bistability

The subject of optical bistability has received considerable efforts for the past fifteen years, because bistable optical devices not only are the basic binary optical elements but also can function as optical switches, optical amplifiers, and optical logic elements. Conventionally, all optically bistable devices have attracted more attention because of their potentials for ultrafast switching capability Currently, the attempt to achieve all optical type devices has encountered serious material problems, i.e. no material shows such a large intrinsic optical nonlinearity to implement a device. Optoelectronic type bistable devices have drawn strong interest recently, since many semiconductor materials show optical nonlinearities (Haug 1988, Ryvkin 1985), and the current semiconductor technology has been developed sufficiently to fabricate devices of extremely small size.

The materials tested to achieve the bistable devices are semiconductors, atomic vapors, liquid crystals and hybrid electro-optical systems. Since there are many good review papers and books (ex. Gibbs 1985) available, the conventional schemes of optical bistability will not be described here. The optoelectronic bistable devices with negative resistance effect will be categorized according to operating mechanisms.

The negative resistance effect (NRE) combined with optical properties is drawing strong interest because of its capability of fast switching, its strong nonlinearity and current progress of semiconductor fabrication technology. Both S-type and N-type NRE have shown good potential for optical switching (Taylor et.al. 1986, 1987, Aleksandrov et al. 1987, Crawford et al. 1988). The N-type NRE gives faster response and less power consumption than the S-type NRE device because of low light absorption at high voltage state. Therefore, for passive optical elements the N-shaped current-voltage characteristic is more attractive. The S-type NRE electronic device is expected to show slower response time than the N-type because of the charge recovery time from high to low current state. However, it shows strong optical response (Sasaki et al. 1985, Taylor et al. 1987) and has the ability to drive other devices. A thorough comparison was made for active and passive optical bistability in semiconductors by Adams (Adams et al. 1985)

A simple way of getting an N-type I-V characteristic is by putting a photosensitive material in the Fabry-Perot resonator (Ryvkin 1981), which uses the refractive index dependence on the absorbed radiation power. But the need to use coherent light somewhat limits its applications.

per call

Recently, N-shape I-V characteristic is achieved with a simple double heterostructure, which is based on electro-absorption effect (Ryvkin 1985). Similar N-shape I-V characteristic has been obtained in multiple quantum well (MQW) structures (Miller et al. 1985, 1986). From phenomenological point of view, the feasibility of the N-shaped current-voltage characteristics is the same in both cases. In quantum well structure the quantum confinement increases the coulomb interaction of the electron and hole, and also increases the exciton binding energy, so the optical absorption corresponding to the exciton resonance remains strong even at room temperature. Another new optoelectronic scheme for optical bistability is a phototransistor with built-in light emitting diode, which is based on the principles of the operation of the so-called camel diode or the bulk barrier. This scheme has shown strong optical response and integrability.

The optical bistability related to negative resistance effect are categorized into three types of optoelectronic bistable devices according to operating principles. The operating principles are explained in the following subsections.

Electroabsorption effect

The electric-field dependence of optical absorption near the band edge in semiconductors has been known for a long time. Not many device applications, however, have been reported. Recently electroabsorption effect has drawn strong attention since D. Miller reported large red-shifted absorption in quantum well structures (Miller et al. 1985). The Stark effect is the reason for the shift of the exciton absorption to lower photon energy. The basic theoretical studies of the electro-absorption effect have been done by Franz and Keldysh independently in 1958. The mechanism is based on the electron wave function broadening by electric field. Their results were extended to photon energies greater than the band gap by Bulyanitsa, Callaway and Tharmalingam (Bulyanitsa 1960, Callaway 1963, Tharmalingam 1963). The electroabsorption effect has also been observed in gallium phosphide, which is related to the bound exciton at nitrogen level (Glinskii 1982).

Up to the present the electroabsorption effect in multiple quantum well (MQW) and double heterostructure (Aleksandrov et al. 1987, Nemenov et al. 1984, Ryvkin 1981) have been applied to optical devices. Both use external serial resistor to provide electric feedback which respond to the photocurrent change. An intrinsic layer is built in between p and n so as to have high electric field region. GaAs edge absorption shifts to lower frequency side due to strong electric field. In the MQW the quantum confinement increases the coulomb interaction of the electron and hole, and also increases the binding energy of the exciton, so the number of electron-hole pairs are increased considerably in the quantum well structure. So does the optical absorption corresponding to the exciton resonance. Therefore, the absorption by the Stark shift of the exciton level and absorption

broadening due to field ionization are increased at lower photon energy. At around bandgap photon energy illumination the MQW structure shows much stronger red-shift than the double heterostructure. At photon energies not close to the band-gap energy both show weak oscillating phenomena.

Bulk Barrier

Bulk barrier is also called camel diode because it has a hump in the band diagram. The shape of energy band is similar to a bipolar transistor, but its operation principle is significantly different. The structure is that highly doped p-layer is sandwiched by two lightly doped n-type layers. The central highly doped p^+ region is normally thin in order to be depleted even at zero bias. Its I-V characteristic is nearly exponential in both directions. However, it is strongly asymmetric if the doping concentrations in the two n-type layers differ by some orders of magnitude even in homojunction case. In the heterojunction case it is strongly asymmetric even with the same doping concentrations because of the bandgap difference.

If photons of bandgap energy are illuminated on active layer (reverse biased n-layer), the photogenerated holes are collected in the valence band of the bulk-barrier layer, which acts as a potential well for them. The holes reduce the electrostatic charge of the acceptor atoms leading to a reduction of the potential barrier. As a result of the lowering of the potential barrier the electron flow from the emitter to the active layer increases. If the electric field in the active layer is high enough to generate secondary electrons by collision, the positive feedback phenomenon occurs between the hole current and the electron current. The breakdown occurs when the hole current generation by collision in the active layer exceeds the hole current flow into the barrier. It will reach a stable state if the internal current gain falls below unity.

Sasaki et.al and Taylor et.al. used this technique for their InGaAsP/InP and GaAs/AlGaAs heterostructure devices, respectively (Sasaki et al. 1985, Taylor et al. 1987).

Space Charge Effect

The negative resistance effect related to the space charge effect in high resistive material was studied in 1960's by Lampart, Ashley and Milnes. A material, which has a deep trap level with capture cross-section asymmetry, will show negative resistance effect if electrons and holes are injected. For example, if assumed that the trap has larger electron capture cross-section than hole capture cross-section, the current is mainly hole current and the bulk is neutral at first. The number of traps occupied by electrons increases gradually, and builds up space charge region locally. The lifetime of electron increases corresponding to the decrease of the density of empty trap sites. On the other hand the hole life time decreases. At certain injection level the electrons

obtain enough kinetic energy to ionize the trapped electron by collision. Electron current and hole current dramatically increase to result in a negative resistance effect.

Now, how can these N- or S-type optoelectronic properties be applied to optical bistable devices? Devices with electroabsorption effect exhibit an N-type I-V characteristics (Aleksandrov et al. 1987, Miller et al. 1985, Nemenov et al. 1984). Devices of the N-type I-V curve have a power advantage, so they are appropriate for application to passive elements. Devices based on bulk barrier and space charge effect show the S-type I-V curve (Sasaki et al. 1985, Taylor et al. 1987). The S-type consumes more power but shows strong optical response, gain and the ability to drive other devices, so it is suitable for an active element.

For passive type elements the signal light transmission changes due to absorption change in the device. To have a positive feedback proper photon energy and bias voltage should be chosen. As an example, consider a device with absorption coefficient like in Fig. 1-1(a). A load line is selected to have two stable operating voltage V_1 and V_2. The wavelength of input light is selected to have maximum absorption at the voltage V_1. The absorption of input light at V_1 is high and the device gives low output intensity. The operating point will stay there until a small perturbation, but large enough to overcome Δi, is provided either in electrical or optical form. If an optical perturbation is applied to the device, the device i-V curve shifts to the left and voltage drop at the device increases to the voltage V_2 because the stable operating point moves along the load line. The absorption peak shifts toward longer wavelength. As a consequence the absorption at the device decreases, and more voltage will be applied to the device since the voltage across the load resistor decreases. The device i-V characteristic curve will be stabilized at a certain position between the two curve in Fig. 1-1(b). At point V_2 the electric field in the device is so high that the absorption of input light in the device is small. A large output signal can be obtained. When the input signal disappear, the operating point moves back to the point V_1 since the operating point can not exist on negative resistance region.

For the active negative resistance device the input signal is only for the purpose of triggering. The output light signal is independent of the input intensity except at the transition moment. Electric bias and a load resistor decide the stable operating point output light intensities. The input light intensity must be large enough to provide the voltage difference between the voltage of low operating point and the breakdown voltage. For instance, assume an optoelectronic device with the properties as in Fig. 1-2. Input light will increase the device current and shift the i-V curve to the left. As a result the operating current of the device jumps from low (i_1) to high (i_2) and so does the output signal intensity. The input light intensity required to turn on the device is correlated to the applied bias voltage.

A high resistivity single crystal like gallium phosphide (GaP) shows large photoconductivity gain for bandgap radiation. Gains in some cases exceed 10^4 for fields of 10^3V/cm (Goldstein 1966). The photoconductivity is strongly influenced by traps. The III-V compounds have shown sensitized photoconductivity when they are doped with electronically active centers. Cu and Ce act as photosensitized centers in GaP (Schulze 1974, Popov et al. 1978). GaP:Cu has shown both enhancing and quenching capability depending on photon energy. In the presence of band-gap radiation, simultaneous infrared radiation can produce various combinations of transient increases and decreases in the photoconductivity depending on the respective light intensities and the specific infrared energy. Some combination of fundamental excitation and quenching transitions is apparently involved. GaP also shows tunnelling effect and avalanche type breakdown phenomenon at low temperature when it is fabricated in light emitting diode. Recently, Soviet researchers reported the negative resistance breakdown phenomena even at room temperature (Anisimova et al. 1977). Another good aspect of GaP LED is that its multi-color emission characteristics according to impurities. It can be used as selective noncontact interconnection element. This implies that, if we understand the roles of impurities and traps in GaP better, many interesting applications are possible in the optoelectronic area.

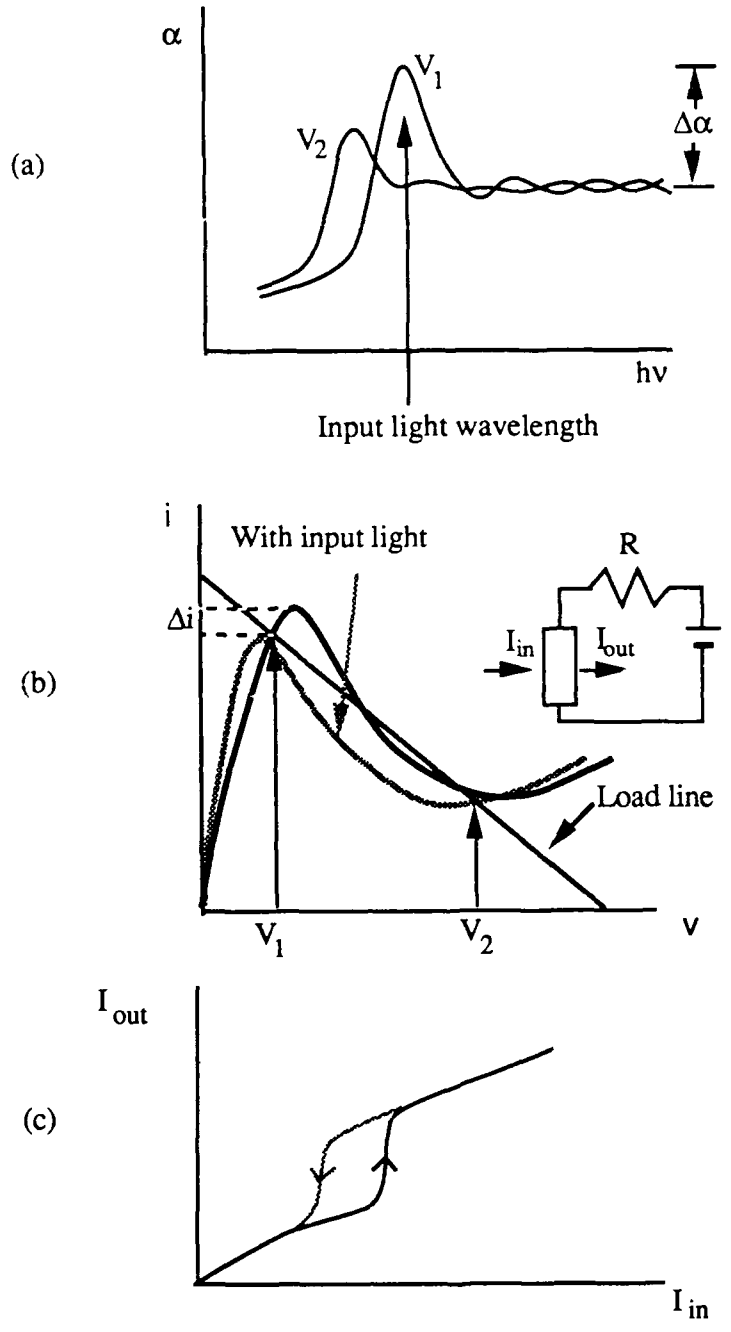

Fig. 1-1 Optical bistability device implement with N-type negative resistance optoelectronic elements. The transmissivity of input light is controlled by the device voltage.

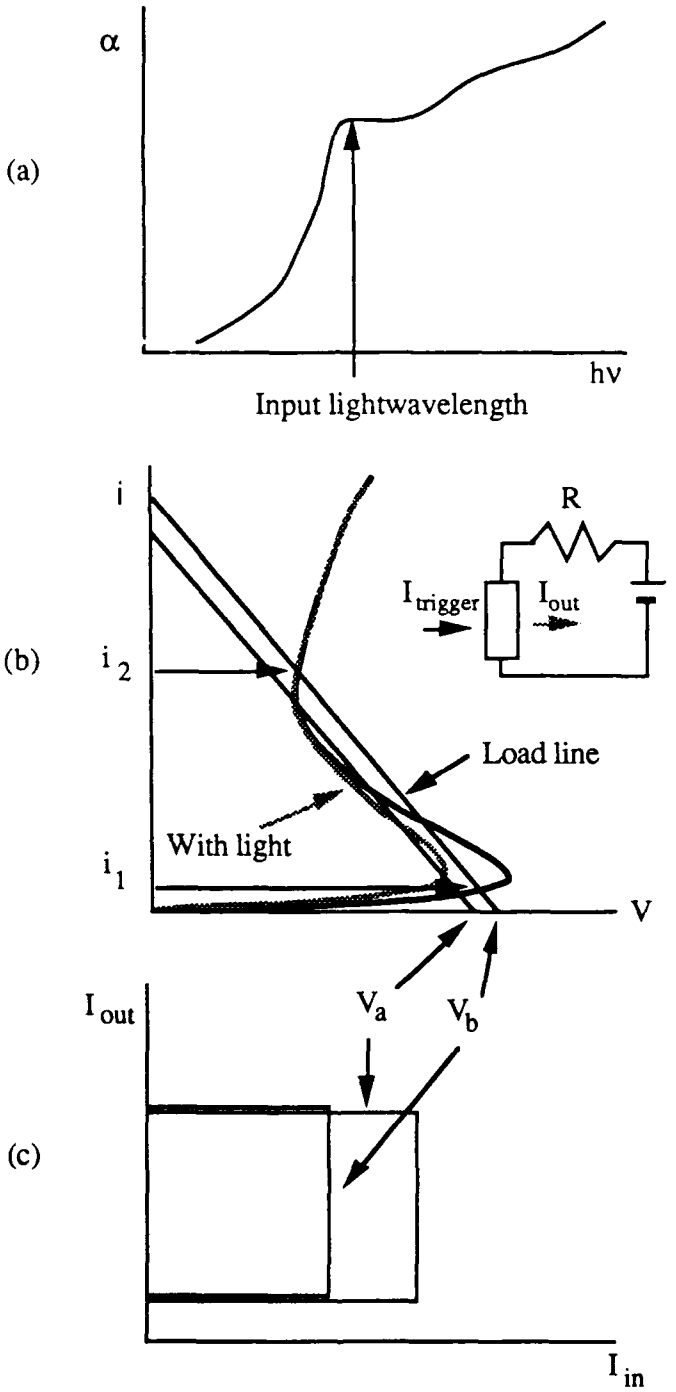

Fig. 1-2 Optical bistability device implement with S-type negative resistance optoelectronic elements. The input light is used to trigger the device and new output light is generated.

Negative Electron Affinity Optically Biased Infrared Detector

The typical infrared photon detection situation is characterized by two distinct photon streams impinging on a detector; background photons and signal photons. The fluctuations in the photon streams produce fluctuations in the detector signal. It is this noise which sets an absolute lower limit for the detection of signal photons. So, we can say that the ultimate goal of the development of infrared detectors is the removal of all the noises unrelated to the photon shot noise.

IR detectors can be classified into two main classes, thermal detectors and photon detectors.

The thermal detectors are based on the changes in the properties of materials resulting from temperature changes caused by the heating effect of the incident radiation. Thus the thermal effects are generally wavelength independent and relatively slow process. Therefore, the thermal detectors show slower response but much wider usable wavelength range than the other type. The radiation thermocouple, the bolometer, the Golay cell and the thermister are comprised in this class.

The photon detectors depend upon photon effects which include all interactions between incident photons and electrons within the material, whether bound to lattice atoms or free. Although there are lots of photon effects, only a few of them are widely exploited. They are photoconductive (PC), photovoltaic (PV), and photoemissive (PE) effects. The PC and PV detectors offer very high detectivities with very fast response in certain range, although they must often be cooled to achieve such performance. The materials being exploited widely are Ge, Si, PbS, PbSe, PbTe, InSb and HgCdTe.

Much of recent research activity on infrared detectors has centered around mercury cadmium telluride (HgCdTe), extrinsic silicon and focal plane array detectors (Albert 1984, Walter et al. 1986). Linear and 2-D arrays are in rapid development. III-V compound superlattices attract much attention recently as an effort to develop new IR technology (Osbourn 1984 and 1986, Hughes 1987). Interest to develop good detectors operating in the ultimate background noise condition motivates to search for novel detection schemes. It is important to investigate the feasibility of different approaches to IR detection, and if such feasibility is established, to follow through with the development of the particular approach.

Now, very efficient low noise visible light detectors with high time resolution are available at low cost, whereas in comparison most IR detectors are expensive, have photon flux thresholds 7-8 orders of magnitude higher and the time resolution is considerably poor. Recently upconversion of IR radiation into visible ranges has been used in order to detect infrared signal (Moser et al. 1985). Upconversion is achievable without introducing distortion into the contained

in the spatial and temporal structure as well as in the frequency spectrum of the initial IR radiation. Thus taking into account all the advantages of the visible light detectors, the upconverters give an impetus to a significant step forward in IR technology. Another important aspect for the infrared upconverter is the strong possibility of achieving room temperature photon detector for infrared signal. So, if we find any system that can convert infrared signal into visible light, we can detect the signal by measuring the up-converted radiation with those good visible detectors. This is the idea of the infrared quantum counter. This basic idea requires a material having several appropriately spaced energy levels. The energy difference between the final state and the initial state must be in visible range. An infrared source of radiation excites the electrons of lower level to intermediate level. Pumping radiation, whose energy is resonant between upper level and the middle level of a three level system, reexcites the electrons at the middle level to the higher state. They then relax to the lower level, emitting upconverted photons or through nonradiative routes.

The upconverted infrared signal can be detected in the form of either upconverted photons or photocurrent. However, in the case of photon detection large portion of the upconverted signal may relax through nonradiative routes. In GaP the nonradiative recombination is larger than the radiative transition. To avoid this problem we must find some ways to detect the signal before it relaxes to the lower levels.

The photoemissive detection techniques are uniquely suited for very high speed detection of low level signal because free photoelectron may be accelerated to a high energy by an electric field and detected as a single event. Appropriate surface treatment is needed to minimize the heating required for electron emission. We generally believe that by the application of cesium and oxygen the conduction band energy level of a wide band gap semiconductor in the bulk is higher than the vacuum energy level of the surface. This is so called Negative electron affinity (NEA) semiconductor surface. NEA semiconductor surface has demonstrated to show a high probability for electron emission into vacuum (Escher 1981). P-type GaP, GaAsP, GaAs, and InGaAsP are commercially used now.

The up-converted infrared signals can be detected by sensitive visible detectors in the form of light or current. The methods can be divided into two types: (1) incoherent interactions like stepwise absorption of infrared and pump photons (Gundersen et al. 1982, 1974) and (2) coherent parametric interaction of infrared and pump electromagnetic waves in crystals or metal vapors resulting in sum frequency mixing (Milton 1972, Herrington 1975). In some case the pumping mechanism is achieved by other means in the type (1) (Moser et al. 1984, 1985).

In this chapter an infrared detector with GaP:Zn,O material is described. The GaP:Zn,O is considered proper for ir upconversion applications because it has a high radiative quantum efficiency, approaching 100% at low temperature (Gershenzon et.al. 1966, Welber et al. 1968) and

the complex impurity level structure in GaP may offer many possibilities for wide range of the linear infrared upconversion. Besides, recent works by Moser et al. in West Germany show a strong possibility of the feasibility of an infrared detector with GaP material. GaP also gives advantage if the upconverted signal is detected by photoemission technique, since wider bandgap material has a tendency to give better photoemission efficiency after cesiation (Escher 1981). The basic principle of this detector is the stepwise excitation of electrons from the valence band to the conduction band of GaP with sequential absorption of infrared signal and optical bias. This scheme requires precise match of bias and signal beam to GaP bandgap energy. In our experiment a low power single mode CO_2 laser is used as infrared signal. The infrared signal is measured in the form of photocurrent and a chamber is designed in order to measure the signal by photoemission technique.

Review of the Infrared Upconversion in GaP

Gundersen et.al. reported efficient infrared upconversion in GaP (Gundersen et al. 1982). Upconversion of 10μm in GaP:Zn,O at 10 K was observed by them through enhancement of a broad emission between 710 and 780 nm. The optical bias was 645 nm. The upconversion efficiency seen in the Zn-O exciton line is larger than 1 %. They also indicated upconversion from several other lines, such as nitrogen, sulphur, tellurium, and bismuth excitons through fluorescence quenching.

The idea of upconversion in semiconductor is obtaining a fluorescence by optical two-step excitation of electrons involving mid gap levels. The intermediate state lifetime determines the requirement on optical bias intensity. Such lifetimes vary considerably, in GaP from ~10 nsec to > 1 sec., depending on impurities. In order for the process to be efficient the ir absorption cross section must be large, and the pump intensity must be sufficient to provide the second excitation step before recombination occurs,

$$n \geq 1/\sigma\tau$$

where n is the number of bias photons per cm^2 sec^{-1}, σ is the absorption cross section of the optical bias and τ is the lifetime of the intermediate state. For the efficient device it is typically necessary that infrared absorption length be comparable to the carrier diffusion length. Typical diffusion length in GaP is micro order.

Moser et al. have observed infrared to visible up-conversion in GaP LED at low temperature(T<40 K). The energy difference between infrared and visible photons is supplied by the electrically injected carriers, not by a pump laser. The observed photoresponse was found to be caused by the ionization of shallow donors only, showing a peak sensitivity of 20 mA/W at 13-μm wavelength (Moser et al. 1984, 1985).

Photoconduction Measurement of the Up-converted Infrared Signal

A simple way to detect the upconverted infrared signal is to observe the luminescence spectra. For GaP:Zn only a few percent of the electrons in the conduction band are expected to recombine radiatively. Most of the upconverted carriers are wasted through nonradiative routes. In order to avoid this signal loss, the photocurrent measurement by contacting a probe direcdy on a sample surface has been tried. In photoconductivity experiment an important factor that affects the upconverted signal is the distance the electrons have to travel. There is a greater probability of recombination if the electrons have to travel a relatively long distance. The electron lifetime in Zn doped GaP is about several 10 nsec at room temperature (Bacharach et al. 1972). The carrier recombination is not only to reduce the signal current but to increase the noise power. The photoconduction technique may be more sensitive to the sample surface condition but the stronger signal response is expected if the surface is properly treated.

Sample preparation

GaP:Zn samples with ohmic and Schottky contacts were prepared for the photoconductivity measurements. The ohmic-contact sample has large noise current that is about 3 orders of magnitude larger than that of Schottky-contact sample, and has much less optical sensitivity than that of the Schottky-contact sample, suggesting that the ohmic contact is not proper for this experiment. Two Schottky-contact geometries were tested; point contact and digitized plane contact. Fig. 1-3 shows these two configurations.

Each sample was attached to the Heli-tran cryogenic cooling system with a low temperature conducting epoxy. The barrier height of p-GaP-Au contact is about 0.7 eV. We can consider the silver epoxy contact as a silver contact. A brass wire was used as the point contact. Double Schottky barrier formed in both cases. In point contact case we can define the forward bias as contact wire being negative with respect to the sample holder. For the plane contact case we cannot define the forward bias since both contacts are exposed on the same surface, but there is a certain direction preference because of the sample surface inhomogeneity.

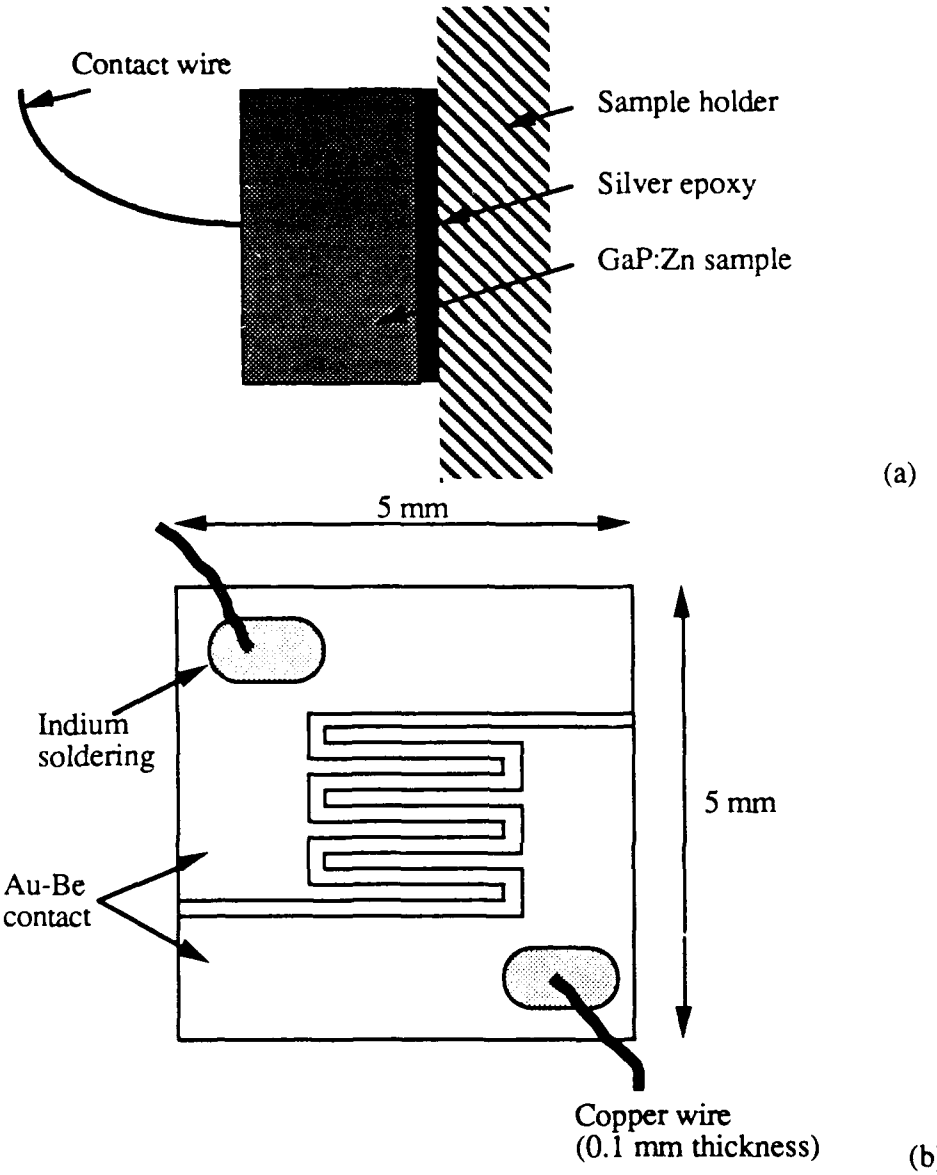

Fig.1-3. The sample metal contact for photoconducting experiment. The width of the exposed area in (b) is 100 mm. (a) is a point contact sample and (b) is a digitized plane contact sample.

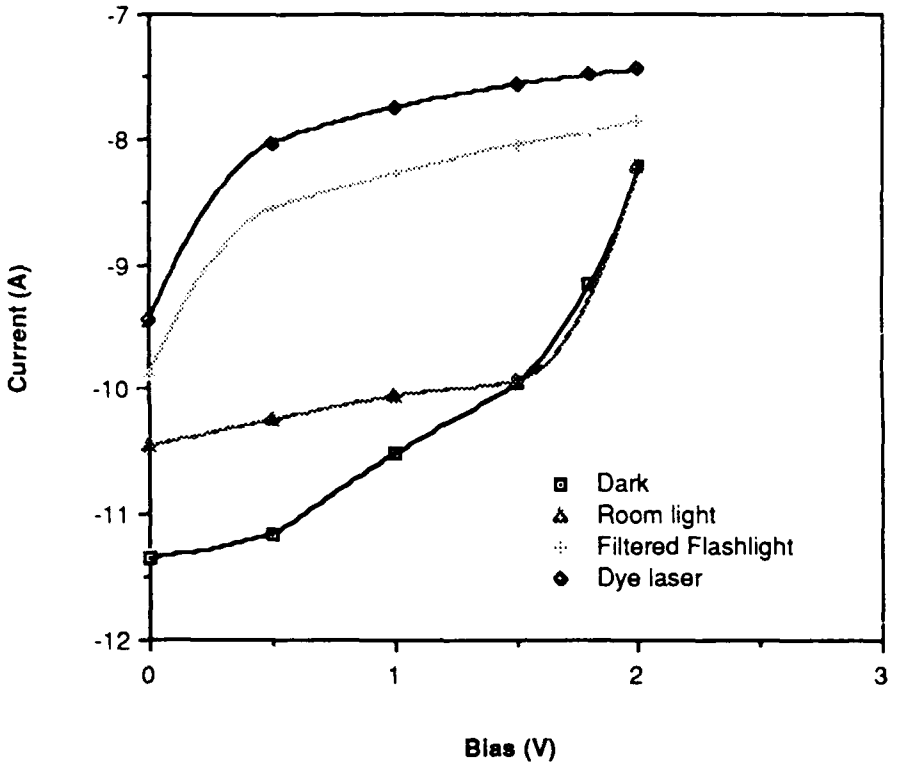

Fig. 1-4. Photocurrent vs. bias voltage under different illumination conditions. The photo response is very sensitive, but shows wide range of optical response which will give large pumping beam noise.

In order to know the proper operating temperature and bias voltage, the sample I-V characteristics were studied. The Keithley Electrometer was used since the sample resistance is in giga-ohm range. The resistance of the plane contact sample is 260 MΩ at one polarity and 3.6 GΩ at reversed polarity at liquid nitrogen temperature with room light. For the point contact case the sample resistance is about 10 GΩ at the reverse bias condition. The sample resistance did not remain constant during experiment. After operating for certain times the resistance changes to 340 MΩ and 1.8 GΩ, respectively in the plane contact case. It seems to be trap related phenomenon. The sample shows better visible light sensitivity at the higher resistance connection. The photo-current change according to the bias is shown in Fig. 1-4. The filter for the flashlight was 570-nm bandpass interference filter. The pumping beam wavelength of the dye laser was 550 nm with the energy of 0.4 mJ per pulse.

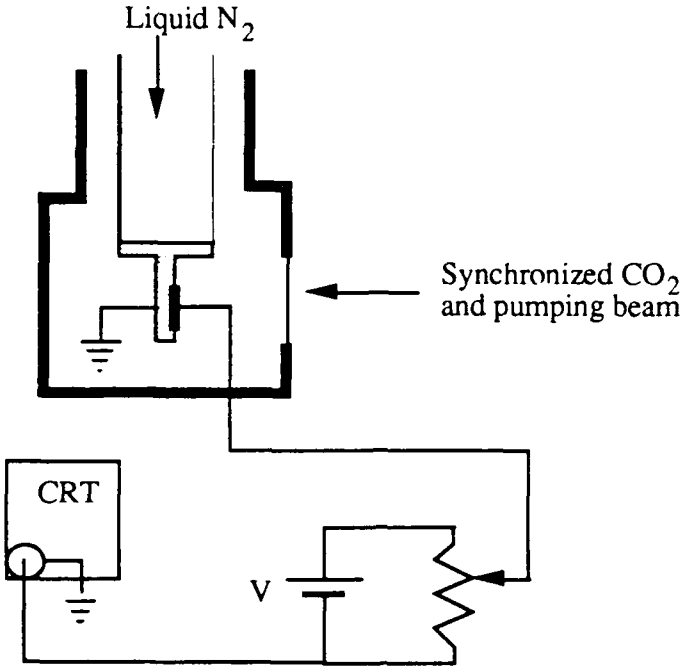

Fig. 1-5 Photocurrent measurement setup for point contact sample. For plane contact sample, both contacts were on the same surface of the sample.

The measurement setup for the point contact samples is shown in Fig.1-5. Weak signal has been observed for the point contact sample but could not discriminate signal from noise for the plane contact case. The plane contacted sample shows stronger photoresponse by about an order than the point contacted one for all visible region as expected. The shorter carrier transit time between electrodes and more absorption in higher field region give better photosensitivity in the plane contact case. For a perfect sample the plane contact is considered to show better signal than the point contact. Here the perfect means that there is no other unwanted impurity level in the bulk and no defect on the sample surface except some dangling bonds. With current technology it is very hard to control impurity concentration, especially deep impurity, on our will. So, the exposed surface area may be depleted by capturing charges from the environment. This probably cause strong noise current. This is the reason why a large noise current appeared by pumping beam.

Analysis of Photoconduction Measurement

The infrared signal current could not be observed in the digitized plane contact sample. The depleted surface states and related trapping by these states may be the reason; most of the current flows along the surface, and generation and recombination on the sample surface results in a short diffusion length.

In the point contact sample the electric field lines are directed toward the sample holder through the bulk region, and thus the recombination effects of the surface states are negligible. In the point contact the illuminated junction is reverse biased. In a dark condition the voltage reading on the scope is

$$V = \frac{-R_i}{R_i + R_d} V_a$$

where R_d is GaP:Zn sample resistance and R_i is the scope input resistance. When the IR signal irradiates on the sample, Zn acceptors capture some of the photoexcited electrons. The holes generated by the IR signal are swept away by the electric field and leave negatively charged acceptor ions near the interface. Some hot carriers in the metal side are also expected by light illumination and this leaves more positive charges near interface. Hence, the voltage drop at junction increases because of the barrier height increase. The mechanism is explained visually in Fig. 1-6.

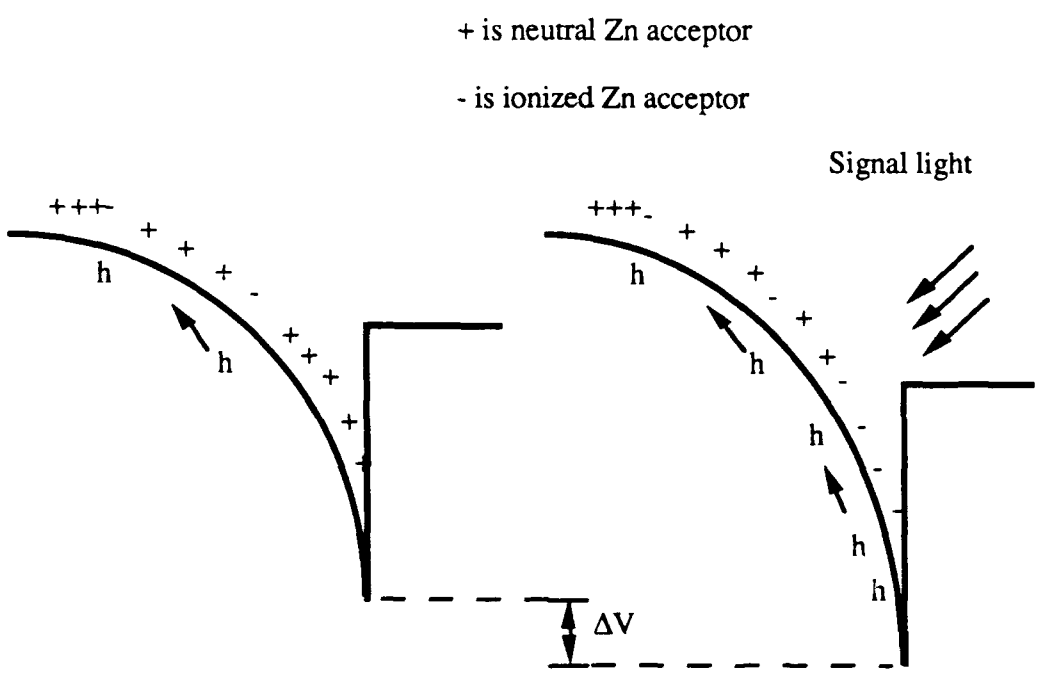

a) In dark b) With infrared signal

Fig. 1-6. In dark the - signs indicate the acceptor sites charged by the thermally generated electrons

Ideally, with only the pump beam illuminating the sample, the photocurrent should not deviate too much from the dark current. However, when the sample is illuminated with both the IR signal beam and the pump beam, the acceptor sites are ionized IR signal and the pump beam

neutralizes the ionized acceptor level by photoexciting the electrons to the conduction band. The increase in carrier concentration should give large voltage reading on the scope.

Experimentally, the dark current was 24 nA at the temperature of 80K. With pump beam alone, the current was 30 nA. With both beams irradiating the sample, the current trace showed some indication of IR signal. The infrared signal current was less than .5 nA. This dark current is much larger than the photocurrent, thus the signal-to-dark current ratio is very small. Therefore, the signal is hard to be detected without removing this noise current. The major dark current sources may be the impurity conduction via surface states and the thermally generated holes. We believe that all those semiconductor noise can be removed by detecting the upconverted electrons at outside bulk. The photoemission experiment will significantly reduce the dark current and improve the signal-to-dark current ratio.

Noise in GaP:Zn,O Infrared Detector

The expected major noise sources are ambient radiation noise and photon noise. Some semiconductor noises such as Nyquist, G-R, and shot noise will be also considered as noise factors in photoconduction technique, but their effect except shot noise will be negligible since the device is very small and operated in cool temperature. Two photon noise by pumping beam can be expected because of the very high concentration of zinc atoms and some deep levels.

Normally GaP has unwanted oxygen impurity level at about .9 eV below the conduction band. This may give more trouble than Zn level for two photon noise, because its energy level is located about in the middle and also make another trap level, Zn-O isoelectronic complex, at about .3 eV below the conduction band. Henry and Lang (Henry et al. 1977) reported that the optical cross-sections from the valence band to oxygen level and from oxygen level to the conduction band are about 10^{16} cm^2 and they are peaked at 1.8 eV, then show slow decreasing trend when energy increases. Zn-O complex also shows big absorption coefficient from the valence band to its energy level at about 2.2 eV, but the absorption from Zn-O associates to the conduction band is negligible. Zn-O associates may affect sensitivity more by capturing electrons from the conduction band rather than two photon noise. Although their concentration is much less than that of zinc, oxygen concentration should be reduced to get better sensitivity and noise-to-signal ratio.

Kopylov et al. reported the absorption coefficient of zinc level in GaP (Kopylov et al. 1978). It is peaked at 56 meV for a GaP:Zn sample with zinc concentration of $5 \cdot 10^{17}$ cm^{-3} and shows decreasing trend according to energy. The energy separation decrease between the conduction band and the acceptor level due to high doping concentration requires very low temperature to remove thermal noise effect.

However, no indication of two photon noise has been detected yet. When we observed the photocurrent response in respect of temperature with pumping beam alone, there was no indication of photocurrent saturation. If the two photon noise is dominant at lower temperature, the current change trend should not be the same as that of dark current. In our observation the current change ratio was almost same. This implies other noise factors are more seriously influencing than two photon noise.

Estimation of the Photoemission from GaP:Zn NEA Infrared Detector

The photoemission processes are usually described by three steps. These steps are

(1) the excitation of the electron with the absorption of the photon energy from the valence band to the conduction band

(2) the transport of the excited electron to the surface

(3) the escape of the electron from the confines of the solid into vacuum.

The approach here will follow the above three steps and other unintentionally doped impurities will not be considered.

Electron Excitation

The GaP samples are heavily Zn doped and two beams, whose photon energy sum matches the bandgap energy, are used to excite electron from the conduction band to the valence band via Zn impurity level. The average number, n_{Zn}, of excited electrons at zinc level by infrared signal and thermal effect is

$$n_{Zn}(x) = \frac{\alpha_{Zn} I_s(x)}{h\nu} \tau_{Zn} + \frac{N_{Zn}}{1+exp[(E_f-E_{Zn})/kT]}$$

where α_{Zn} is the absorption coefficient of Zn, I_s is infrared signal intensity and τ_{Zn} is the lifetime of the excited electron. The second term must be kept small. The absorption cross section calculated from the absorption coefficient data (Kopylov 1978) is $2 \cdot 10^{-16}$ cm^2 at CO_2 wavelength. The value will vary with doping concentration. The number of upconverted electrons, n_p, in the conduction band is given by

$$n_p = \frac{\sigma n_{Zn} I_p(x)}{h\nu} \tau_e$$

where σ is the optical absorption cross section of Zn acceptor, I_p is pumping beam intensity, and τ_e is the electron lifetime in the conduction band. The measured minority carrier lifetime in GaP:Zn is about 20~40 nsec (Bachrach 1972).

Electron transport, workfunction lowering and escape depth

Some elementary considerations are necessary to understand the crucial role of the transport process. An electron, after photoexcitation from the valence band may or may not reach the surface and escape. The probability depends on energy losses due to inelastic scattering involving other electrons, impurities and phonons. These inelastic scattering events give an electron mean free path 50~100 Å (Escher, 1981). The pumping beam exactly matches the energy difference between the conduction band and the zinc level. The potential barrier to escape to the vacuum is too high to overcome. The position of the valence band maximum of GaP is about 6 eV below vacuum (Laar et al. 1977). Hence, the work function lowering process is necessary to get photoemissive electrons out of the crystal with the light of its band-gap energy.

In recent years, remarkable improvements in the photoemission from semiconductors have been obtained through deliberate modification of the energy-band structure. The approach has been to reduce the electron affinity, E_a, and thus to permit the escape of electron which have been excited into the conduction band at greater depths within the material. Most efforts have been done with Alkali metals because Alkali metals have relatively lower work function than others. Among them the most red-sensitive is cesium which is widely used in the activation of most commercial phototubes. Cesium or cesium oxide compound adsorption can lower the work function energy. This is well known thing even though there still remains uncertainty about mechanisms. Cesium is unstable in air and its fusion temperature is about 302 K, must therefore keep in the vacuum during experiment. The energy band diagram is shown in Fig. 1-7 after cesiation.

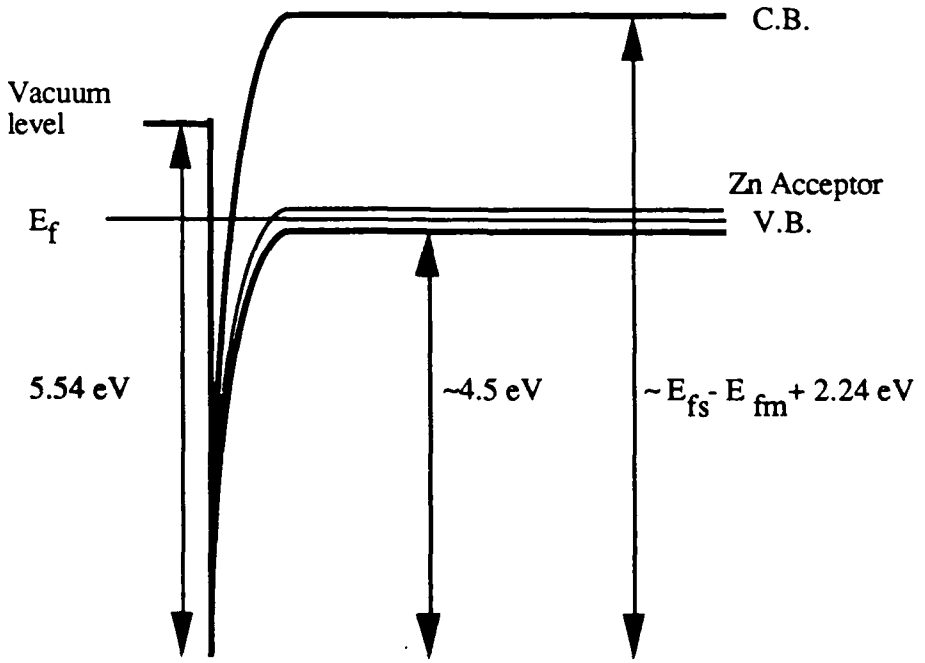

Fig. 1-7. The energy band diagram after cesiation. The work function of Cs is assumed as 1 EV.

The quantum yield near threshold, Y, can be described by (Escher et al. 1973, Martinelli 1974)

$$Y = \frac{B\sigma n_{Zn} L (1-r)}{1-\sigma n_{Zn} L}$$

where L is the electron diffusion length, B is the surface escape probability, and r is the reflectivity of the GaP surface. The quantum efficiency of 10^{-3} has been obtained with bandgap light for a p-GaP:Cs sample of 10^{18}-10^{19} cm^{-3} concentration (Martinelli 1974).

Photoemission Experiment Setup

An ultra-high vacuum chamber is designed as a general test bed for photoemission experiment and testing of materials. This chamber is constructed for the specific purpose of allowing easy access for optical alignment and sample cooling.

Chamber design

The vacuum system is a moderate size of 304 stainless steel with several feedthroughs for pumping, cesium and oxygen inlets, instruments and access. The top cover is demountable. In this way we are able to access heater, sample and all the inside connections of the feedthroughs. Fig. 1-8 shows a side view of the vacuum chamber and Fig. 1-9 is the top view. A modified Heli-tran cold end is mounted on the top cover and a sample holder is attached at the end of the cold end. The original Heli-tran cold end was designed to use up to the high vacuum condition. Ceramic plates cover both side of the sample holder except the area for sample attachment. These ceramic plates prevent the sample holder from excessive heating during sample cleaning, and also block radiational heat exchange between the sample holder and chamber wall. The chamber is cylindrical shape and measures 8" diameter by 8" height. For optical access one quartz window for pumping beam and a self designed NaCl optical window are installed with 15 degree tilt from the normal of the sample surface, respectively. A problem with the current design is that the Torr seal used for infrared window vacuum seal may not withstand the ultra-high vacuum condition. The vacuum condition at the infrared window section can be improved by using viton O-ring seal with a small size extra ion pump.

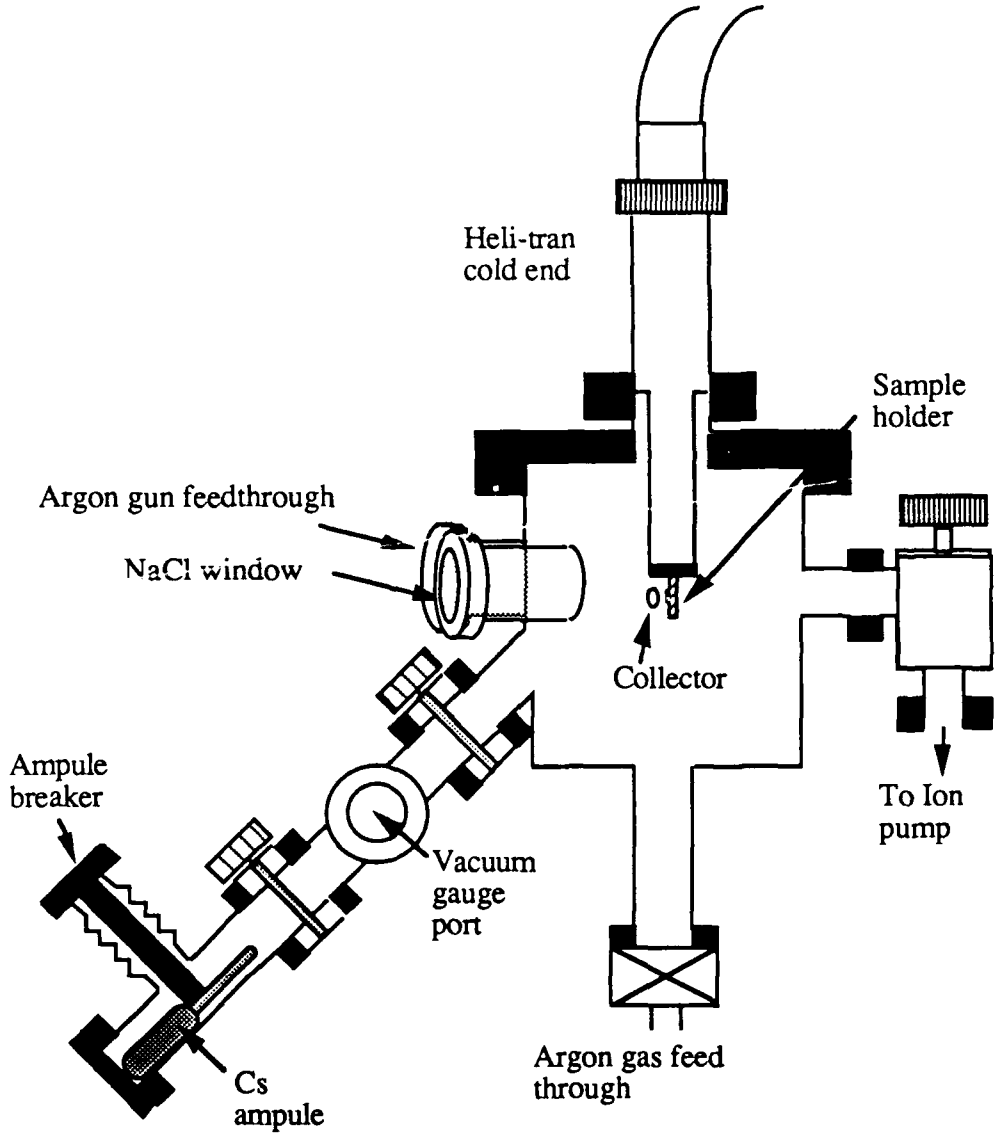

Fig. 1-8 A side view of the main chamber and Cs chamber. A heater is surrounded NaCl window to blow away moisture. The collector for photoemitted signal is mounted on linear motion feedthrough not to interrupt sample cleaning.

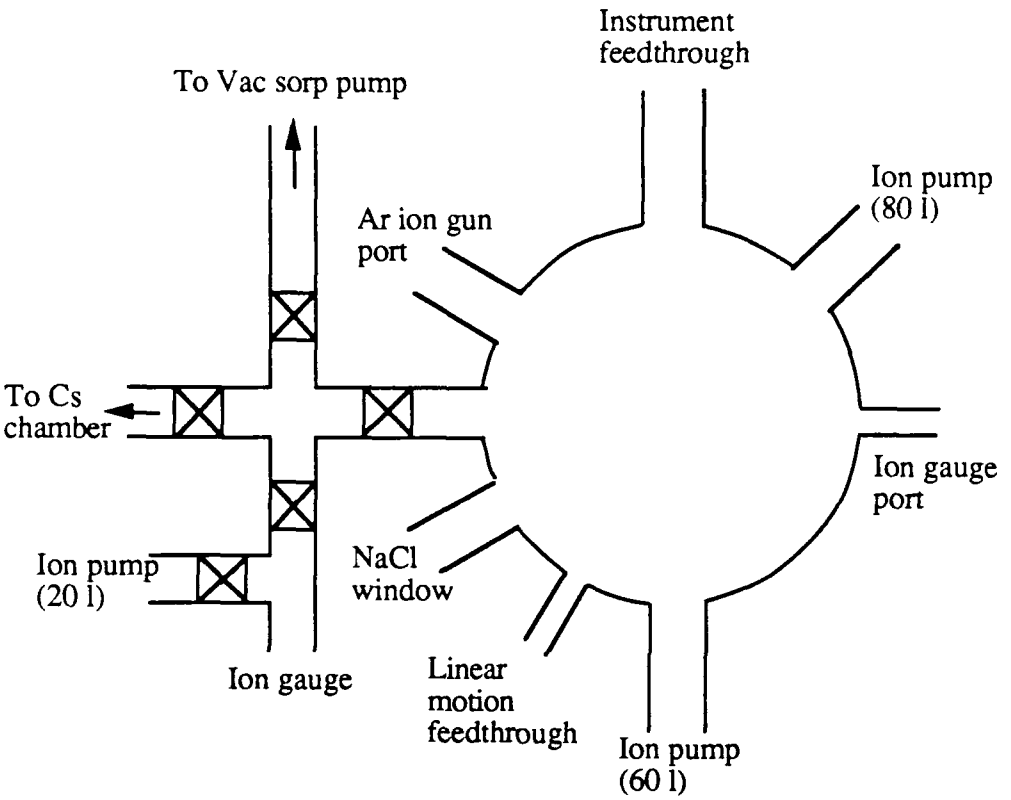

Fig. 1-9. Top view of the vacuum chamber.

Surface cleaning

The GaP(111) surface was cleaned in the ultra high vacuum chamber by Ar-ion bombardment. Residual air molecules will affect the cleaning. The time required to form a monolayer of adsorbed air molecules is $t = \sqrt{2\pi mkT}/(\alpha\pi r^2 P)$. Where r is the radius of the air molecule, P is a chamber pressure in Torr, m is the weight of air molecule, and α is sticking coefficient. At T=293 K and $P=10^{-9}$ Torr, the time for monolayer formation is about 42 minutes with the assumption of $\alpha = 1$. We need at least 10^{-9} Torr to have proper working time. The initial pressure in the chamber is below 10^{-9} Torr and then filled with research grade (purity 99.9998%) Ar gas to 2×10^{-5} Torr. The gun operated for 10 min. at 1000eV, 3μA. The estimated etching thickness is about 200 Å. The surface may be damaged by the heavy Ar ion bombardment, and needed annealing.

Cesiation

A cesium ampule crusher is installed in a chamber attached to the sample chamber and the two chambers are separated by an ultrahigh vacuum valve. A 99% purity Cs ampule is located in the Cs chamber and evacuated below 10^{-8} torr. And then the ampule is crushed by the crusher, which is vacuum sealed by a bellow, and reevacuated below 10^{-6} torr because the ampule is filled with 1 atm of argon gas. The best vacuum we can get was 10^{-6} Torr because the vapor pressure of cesium is about 10^{-6} and 10^{-7} Torr at room and freezing temperature, respectively. The cesium flux is monitored through a cold cathode vacuum gauge which is attached in between the cesium chamber and the main chamber. The cesium chamber and the cesium flow route are heated up to 320K. The vapor pressure of Cs at 320K is 10^{-5} torr. The reported optimum Cs dosage is about $5\cdot10^{14}$ cm^{-2} (Bommel et al. 1980).

Detection circuit

To collect the photoemitted electrons 1KV is applied to the ring shaped collector. The circuit is shown in Fig. 1-10.

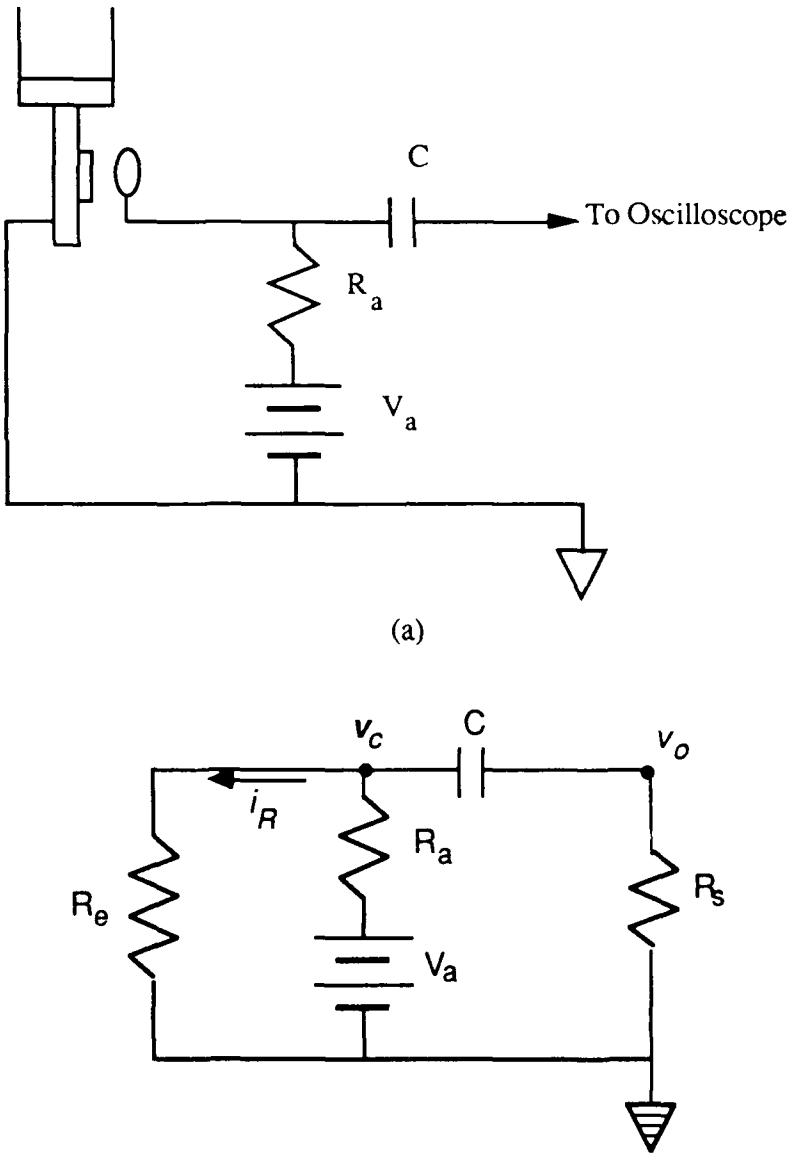

Fig. 1-10. (a) is collector circuit and (b) is equivalent collector circuit: R_e is the equivalent resistance between the ring collector and the sample holder, i.e. R_e = collector voltage/photocurrent , R_S is the input resistance of the oscilloscope.

Initially the capacitor is charged with 1 KV since i_R is negligible in dark condition. The output voltage v_O is zero. When light pulse radiates on the sample i_R is no longer zero. The first restraint on the response is the voltage across the capacitor must remain invariant. The new initial current through the capacitor, i_C is determined by R_a, R_e, and R_S.

$$i_c = \frac{V_{eq} - v_c(0)}{R_s + R_e // R_a}, \text{ where } V_{eq} = \frac{R_e}{R_a + R_e} V_a$$

And by using $i_C(0)$ we obtain the new initial output voltage, $v_O(0)$ is

$$v_O(0) = i_C(0) \cdot R_S .$$

The time constant τ is

$$\tau = C(R_S + R_e // R_a).$$

Hence, the transient response of the output signal is

$$v_O(t) = v_O(0) \exp(-t/\tau).$$

In experiment, R_e is much larger than R_a because i_R is very small quantity. For example, if i_R is in nano ampere range , then R_e is in hundred giga-ohm range. So the output signal is approximated as

$$v_O(t) \cong - i_R R_S \exp(-t/\tau).$$

The output voltage is approximately proportional to the photocurrent i_R and R_S. Increasing R_S will provide larger output signal but slower response is expected because large R_S increases τ..

Conclusion

To detect upconverted infrared signal the photoconducting scheme has been tried. In this case the noise current by the pumping beam and imperfect surface state is too dominant to see the signal since the probe is directly contacted on the sample. The indication of infrared signal could be observed, but it is too weak to estimate the quantum efficiency. The sample surface defects and edge absorption due to high impurity concentration are to be the reasons. Although the surface defects due to dangling bond and the band tailing effect are probably inherent in the system, it can be minimized by precise selection of the pump beam frequency.

LIST OF PUBLICATIONS UNDER PARTIAL OR FULL ONR SPONSORSHIP DURING THE PERIOD 7-1-86 TO 9-30-89, INCLUDING JOURNAL REFERENCES:

REFEREED PUBLICATIONS:

"A semi-empirical formalism for the calculation of deep level wavefunctions in k space," H-H. Dai, M.A. Gundersen, and C.W. Myles, Phys. Rev. B. **33**, 823 (1986).

"Measurement of excited-state densities during high-current operation of a hydrogen thyratron using laser-induced fluorescence," D.A. Erwin and M.A. Gundersen, Appl. Phys. Lett. **48** 1773 (1986).

"Phonon assisted indirect recombination of bound excitons in N-doped GaP, including near resonant processes," H. Dai, M.A. Gundersen, C. W. Myles and P. G. Snyder, Phys. Rev. B **37**, 1205 (1988).

"An optoelectronic bistability in gallium phosphide," M.S. Choi, J.H. Jur, and M A. Gundersen, App. Phys. Lett. **52** (19), 1563 (1988).

"Phonon assisted recombination in GaAs/AlGaAs multiple-quantum-well structures", H. H. Dai, M. S. Choi, M. A. Gundersen, H. C. Lee, P. D. Dapkus and C.W. Myles, J. App. Phys. **66** (6), 2538 (1989).

"Avalanche breakdown in p-n AlGaAs/GaAs heterojunctions," J. H. Hur, C. W. Myles and M. A. Gundersen, accepted for publication in J. Appl. Phys.

OTHER PUBLICATIONS:

"Summary of the workshop for research issues in power conditioning, M.A. Gundersen, editor, University of Southern California (1986).

"Preliminary results from the III-V pulsed power device research program at USC," M.A. Gundersen, Proceedings of the Semiconductor Switch Workshop, Norfolk, Virginia, May 23-24, 1988.

"New concepts for accelerator components", M.A. Gundersen, Proceedings of the Workshop on High Luminosity Asymmetric Storage Rings for B Physics, pgs 159-172, Caltech, April 25-28 1989.

"Modeling of the discharge plasma in a Back Lighted Thyratron," H. Bauer, G. Kirkman, J. Kunc, and M.A. Gundersen, Proceedings, Seventh IEEE Pulsed Power Conference, Monterey, California, June 11-14, 1989.

"Design of an opening and closing GaAs static induction transistor for pulsed power applications," P. Hadizad, J.H. Hur, M.A. Gundersen, and H.R. Fetterman, Proceedings, Seventh IEEE Pulsed Power Conference, Monterey, California, June 11-14, 1989.

"A GaAs-AlGaAs based thyristor, J.H. Hur, P. Hadizad, M.A. Gundersen, and H.R. Fetterman, Proceedings, Seventh IEEE Pulsed Power Conference, Monterey, California, June 11-14, 1989.

"Avalanche breakdown in p-n AlGaAs/GaAs heterojunctions," Charles W. Myles, J.H. Hur, and M.A. Gundersen, Proceedings, Seventh IEEE Pulsed Power Conference, Monterey, California, June 11-14, 1989.

"A high current density thyristor-like gallium phosphide based optoelectronic switch," S.D. Tsiapalas, J.H. Hur, M.S. Choi, and M.A. Gundersen, Proceedings, Seventh IEEE Pulsed Power Conference, Monterey, California, June 11-14, 1989.

"The back-lighted thyratron", in "Optics in 1989", Optics News **15**. 37 (1989), (invited).

PRESENTATIONS 1986 - 1989:

"Model for Phonon-assisted Indirect Recombination at N-bound Exciton in GaP," H-H. Dai, C.W. Myles, P.G. Snyder, and M.A. Gundersen, Meeting of the American Physical Society, Bull. Am. Phys. Soc. **31**, 504 (1986).

"Semi-empirical Formalism for Wavevector Dependent Deep Level Impurity Wavefunctions in Semiconductors," H-H. Dai, C.W. Myles, and M.A. Gundersen, Meeting of the American Physical Society, Bull. Am. Phys. Soc. **31**, 503 (1986).

"Laser Induced Fluorescence in High Power Switch Research," M.A. Gundersen, ETH, Zurich, Switzerland, May 12, 1986.

"High Power Electronics Research at the University of Southern California," M.A. Gundersen, U.C.L.A., Nov. 24, 1986.

"High Power Electronics," M.A. Gundersen, Quantum Electronics Seminar, University of Southern California, Los Angeles, California, December 2, 1987.

"Optoelectronic bistability in gallium phosphide," M.S. Choi, J.H. Jur, and M.A. Gundersen, 1988 Conference on Lasers and Electro-Optics **59**, 244, Anaheim, California, April 27, 1988.

"Preliminary results from the III-V pulsed power device research program at USC," M.A. Gundersen, Semiconductor Switch Workshop, Norfolk, Virginia, May 23-24, 1988.

"Optoelectronic bistability in gallium phosphide," M.S. Choi, J.H. Hur, and M.A. Gundersen, OPTCON '88 Technical Digest pg 183, Santa Clara, California, Nov. 4, 1988.

"Pulse power research issues", M.A. Gundersen, Investment Strategy Meeting on Pulse Power Technology, Wright-Patterson Air Force Base, March 14, 1989 (invited).

"Avalanche breakdown in p-n AlGaAs/GaAs heterojunctions," Charles W. Myles M. Gundersen, and J.H. Hur, Bull. Am. Phys. Sco. **34** (3), 1001, March (1989), American Physicsal Society Meeting, St. Louis, Missouri, March 20-24, 1989.

"New concepts for accelerator components", M.A. Gundersen, Workshop on High Luminosity Asymmetric Storage Rings for B Physics, California Institute of Technology, April 26, 1989.

"Transient behavior and modeling of optoelectronic bistable behavior in a gallium phosphide LED," M.S. Choi, J.H. Hur, S.D. Tsiapalas, and M.A. Gundersen, Cleo '89, CLEO/QELS '89

Advance Program, 47, Conference on Lasers and Electro-Optics, Baltimore, Maryland, April 24-28, 1989.

"Design of an opening and closing GaAs static induction transistor for pulsed power applications," P. Hadizad, J.H. Hur, M.A. Gundersen, and H.R. Fetterman, Seventh IEEE Pulsed Power Conference, Monterey, California, June 11-14, 1989.

"A GaAs-AlGaAs based thyristor, J.H. Hur, P. Hadizad, M.A. Gundersen, and H.R. Fetterman, Seventh IEEE Pulsed Power Conference, Monterey, California, June 11-14, 1989.

"Avalanche breakdown in p-n AlGaAs/GaAs heterojunctions," Charles W. Myles, J.H. Hur, and M.A. Gundersen, Seventh IEEE Pulsed Power Conference, Monterey, California, June 11-14, 1989.

"A high current density thyristor-like gallium phosphide based optoelectronic switch," S.D. Tsiapalas, J.H. Hur, M.S. Choi, and M.A. Gundersen, Seventh IEEE Pulsed Power Conference, Monterey, California, June 11-14, 1989.

"New research directions," M.A. Gundersen, NATO Advanced Research Workshop on the Physics and Applications of High Power Hollow Electrode Glow Switches, Lillehammer, Norway, July 17-21, 1989.

"A partial summary of pulse power research activities at the University of Southern California," M.A. Gundersen, The Second SDIO/ONR Pulse Power Physics Meeting, San Diego, California, July 25-26, 1989.

A review of the back lighted thyratron and its applications", Sixth Key Technologies Score Group Meeting, Huntington Beach CA, October 23-27, 1989. (invited).

"GaAs based opto-thyristor for pulsed power applications," J. H. Hur, P. Hadizad, S. G. Hummel, K.M. Dzurko, P. D. Dapkus, M. A. Gundersen, and H. R. Fetterman, submitted to IEDM 1989.